PLATELETS AND THROMBOPOIESIS

Oxidized LDL activates blood platelets through CD36/NOX2–mediated inhibition of the cGMP/protein kinase G signaling cascade

Simbarashe Magwenzi,[1] Casey Woodward,[1] Katie S. Wraith,[1] Ahmed Aburima,[1] Zaher Raslan,[1] Huw Jones,[1] Catriona McNeil,[1] Stephen Wheatcroft,[2] Nadira Yuldasheva,[2] Maria Febbriao,[3] Mark Kearney,[2] and Khalid M. Naseem[1]

[1]Centre for Cardiovascular and Metabolic Research, Hull-York Medical School, Thrombosis Research Laboratory (013/014), University of Hull, Hull, United Kingdom; [2]Division of Cardiovascular and Diabetes Research, Leeds Multidisciplinary Cardiovascular Research Centre, LIGHT Laboratories, University of Leeds, Leeds, United Kingdom; and [3]School of Dentistry, University of Alberta, Edmonton, AB, Canada

Key Points

- oxLDL binds platelet CD36 to stimulate tyrosine kinase– and PKC-dependent activation of NOX2 and generation of ROS.
- oxLDL- and hyperlipidemia-induced ROS mediate platelet desensitization to inhibitory cGMP signaling to facilitate platelet activation and thrombus formation.

Oxidized low-density lipoprotein (oxLDL) promotes unregulated platelet activation in dyslipidemic disorders. Although oxLDL stimulates activatory signaling, it is unclear how these events drive accelerated thrombosis. Here, we describe a mechanism for oxLDL-mediated platelet hyperactivity that requires generation of reactive oxygen species (ROS). Under arterial flow, oxLDL triggered sustained generation of platelet intracellular ROS, which was blocked by CD36 inhibitors, mimicked by CD36-specific oxidized phospholipids, and ablated in CD36$^{-/-}$ murine platelets. oxLDL-induced ROS generation was blocked by the reduced NAD phosphate oxidase 2 (NOX2) inhibitor, gp91ds-tat, and absent in NOX2$^{-/-}$ mice. The synthesis of ROS by oxLDL/CD36 required Src-family kinases and protein kinase C (PKC)-dependent phosphorylation and activation of NOX2. In functional assays, oxLDL abolished guanosine 3′,5′-cyclic monophosphate (cGMP)-mediated signaling and inhibited platelet aggregation and arrest under flow. This was prevented by either pharmacologic inhibition of NOX2 in human platelets or genetic ablation of NOX2 in murine platelets. Platelets from hyperlipidemic mice were also found to have a diminished sensitivity to cGMP when tested ex vivo, a phenotype that was corrected by infusion of gp91ds-tat into the mice. This study demonstrates that oxLDL and hyperlipidemia stimulate the generation of NOX2-derived ROS through a CD36-PKC pathway and may promote platelet hyperactivity through modulation of cGMP signaling. (*Blood*. 2015;125(17):2693-2703)

Introduction

Individuals with cardiovascular disease (CVD) succumb to changes in blood plasma composition and vessel wall structure that enhance the activation of platelets and promote pathological arterial thrombosis. In healthy blood vessels, excessive platelet activation is restricted by endothelial-derived nitric oxide (NO) through a guanosine 3′,5′-cyclic monophosphate (cGMP)- and protein kinase G (PKG)-dependent mechanism.[1] However, in subjects at risk of arterial thrombosis, this key protective pathway is overcome, resulting in uncontrolled platelet activity. One major factor that contributes to platelet hyperactivity in CVD is dyslipidemia,[2-4] which is characterized by the accumulation of oxidized lipids in the circulation and vessel walls, primarily in the form of oxidized low-density lipoproteins (oxLDLs). The accumulation of oxidized lipids in the plasma of high-risk patients is associated with increased platelet reactivity,[5] whereas oxLDLs, both generated in vitro and isolated from subjects with CVD, contribute to platelet activation, suggesting that they are potential causative agents for the promotion of platelet hyperactivity in CVD.[6-12] However, given the heterogeneous nature of oxLDLs, the mechanisms by which they promote platelet activity and thrombosis in vivo are likely to be numerous. Interestingly, several diseases associated with platelet hyperactivity have been characterized with hyporesponsiveness to NO/cGMP signaling,[13-15] suggesting that platelet hyperactivity in these disease states may, at least in part, be caused by impaired sensitivity to platelet inhibitors through unknown mechanisms.

CD36 is a scavenger receptor that potentially transduces the effects of oxidized lipids in the plasma into platelet hyperactivity. In mice, dyslipidemia enhances thrombosis in vivo, with the pathological phenotype corrected by deletion of CD36.[11] Consistent with those observations CD36 is required for the activation of human platelets in response to oxLDL through signaling events that include the activation of Src kinases, c-Jun N-terminal kinase, and extracellular signal-regulated kinase.[12,16-19] However, it is unclear how the downstream signaling pathways link CD36 to changes in specific platelet functions. In vascular smooth muscle, CD36 ligation activates the multisubunit

Submitted May 14, 2014; accepted February 3, 2015. Prepublished online as *Blood* First Edition paper, February 20, 2015; DOI 10.1182/blood-2014-05-574491.

C.W. and K.S.W. contributed equally to this study.

The online version of this article contains a data supplement.

There is an Inside *Blood* Commentary on this article in this issue.

The publication costs of this article were defrayed in part by page charge payment. Therefore, and solely to indicate this fact, this article is hereby marked "advertisement" in accordance with 18 USC section 1734.

enzyme complex reduced NAD phosphate oxidase 2 ($gp91^{phox}$/NOX2) to produce reactive oxygen species (ROS).[20] Platelet-generated ROS can enhance platelet recruitment by preformed platelet aggregates,[21] although it is unclear if this is important for oxLDL-mediated platelet activation. We hypothesized that oxLDL could induce the generation of platelet ROS through CD36 to promote platelet hyperactivity. Our data demonstrate that ligation of CD36 by oxLDL stimulates Src-family kinase– and protein kinase C (PKC)-dependent generation of ROS through the formation of an active complex of reduced NAD phosphate oxidase subunits. Moreover, the ROS generated by NOX2 activates platelets indirectly by reducing platelet sensitivity to cGMP signaling. These data present a mode of action by which oxLDL induces platelet activation through the modulation of inhibitory signaling.

Methods

Materials

PP2 and PP3 were from Calbiochem (Nottingham, UK). U73122 was from Tocris (Bristol, UK). $oxPC_{CD36}$ (KoDiA PC), 1-palmitoyl-2-arachidonoyl-sn-phosphatidylcholine (PAPC), FA6-152, anti-PKG, anti-Syk, and anti-PLCγ2 antibodies were from Santa Cruz (Wembley, UK). Phospho-VASP-ser^{239}, phospho-PKC substrate and phosphoSrc-tyr^{418} antibodies were from Cell Signaling (Hitchen, UK). Anti-β-tubulin, anti-phosphotyrosine (4G10), and immunoglobulin G (IgG) control were from Upstate (Watford, UK). Anti-$p47^{phox}$ and anti-$p22^{phox}$ antibodies were from BD Biosciences (Oxford, UK). The ROS/superoxide detection kit for microscopy and microplates was from Enzo Life Sciences (Exeter, UK), and the PKG activity kit was from MBLI (Woburn, MA). All other chemicals were from Sigma (Poole, UK).

Experimental animals

$CD36^{-/-}$ (provided by Prof Maria Febbriao, University of Alberta, Canada), $NOX2^{-/-}$ (The Jackson Laboratory, Bar Harbor, ME), and $ApoE^{-/-}$ mice (Charles River, Kent, UK) and wild-type (WT) littermates were all on C57BL/6 backgrounds. $ApoE^{-/-}$ mice were fed a standard chow diet (Harlan Laboratories, Indianapolis, IN) for 8 weeks, then fed a Western diet (21% fat; 829100; Special Diet Services, Braintree, UK) for a further 8 weeks before being implanted with osmotic minipump animal (see supplemental Method 1 available on the *Blood* Web site) that were prefilled with either gp91ds-tat or gp91ds-tat scrambled to provide a dose of 10 mg/kg per day. They were then fed the Western diet for a further 4 weeks (a total of 12 weeks). WT littermates were fed normal chow for the duration of the experiments.

Platelet aggregation, thrombus formation under flow conditions, and flow cytometry

For the isolation of human and murine platelets, please see supplemental Method 2. Washed platelets (3×10^8 platelets/mL) were incubated with low-density lipoprotein (LDL) at 37°C for 15 minutes, followed by 8-pCPT-cGMP (50 μmol/L) for 2 minutes, and then stimulated with thrombin (0.05 U/mL); aggregation was monitored for 4 minutes using Born aggregometry. For the thrombosis assay, reconstituted blood was used, where platelets (4×10^8 platelets/mL) were stained with $DiOC_6$ (1 μmol/L) for 10 minutes at 37°C and treated with 8-pCPT-cGMP (50 μmol/L) for 2 minutes prior to reconstitution with autologous red blood cells (RBCs) at a ratio of 1:1 (final count 2×10^8 platelets/mL). In some cases, platelets were incubated with oxLDLs (50 μg/mL) for 15 minutes prior to 8-pCPT-cGMP (50 μmol/L) in the presence or absence of MnTMPyP (100 μmol/L), TEMPOL (1 mmol/L), gp91ds-tat, or its scrambled control (2 μmol/L) prior to the addition of RBC. To measure ROS production, platelets were preincubated with a superoxide-detection probe (5 μmol/L) at 37°C for 20 minutes. Reconstituted blood was then perfused through fibrinogen-coated (1 mg/mL) capillary tubes at a shear rate of 1000 s^{-1} for 2 minutes, and images of stably adhered platelets/thrombi were captured as previously described.[22] For the flow cytometry assays, whole murine blood was incubated with 8pCPT-cGMP (50 μmol/L) for 2 minutes and then stimulated with adenosine 5′-diphosphate (ADP; 10 μmol/L) for 10 minutes before fixation with formylsaline (0.2%). Flow cytometry was performed using a BD Fortessa and analyzed for fibrinogen binding.[14]

Isolation and oxidation of plasma LDL

LDL (density, 1.019-1.063 g/mL) was prepared from fresh human plasma by sequential density ultracentrifugation[7] and oxidized with $CuSO_4$ (10 μmol/L) at 37°C for 24 hours before dialysis against phosphate buffer (140 mmol/L NaCl, 8.1 mmol/L Na_2HPO_4, and 1.9 mmol/L NaH_2PO_4 [pH 7.4]) containing EDTA (100 μmol/L) to remove copper ions.[23] The oxidation was determined by relative electrophoretic mobility,[24] which was 1 ± 0 and 3.5 ± 0.9 for native low-density lipoprotein (nLDL) and oxLDL, respectively. Separate preparations of LDL were used to repeat the individual experiments.

Fluorescence microscopy

Glass microscope slides were coated with either nLDL or oxLDL (50 μg/mL) for 12 hours at 4°C. Washed platelets (5×10^7 platelets/mL) were incubated with the stated inhibitors and adhered for up to 60 minutes at 37°C as previously described.[25]

Platelet ROS production

Platelet ROS generation was measured fluorescently. Suspended washed platelets (1×10^8 platelets/mL) were incubated with a superoxide-detection probe (5 μmol/L) in a microplate for 30 minutes at 37°C and then treated with either nLDL or oxLDL (1-50 μg/mL) for 15 minutes, and fluorescence was measured at 650 nm. To allow ROS generation to be visualized, washed platelets (5×10^7 platelets/mL) were preincubated with the superoxide-detection probe and adhered to immobilized LDL (50 μg/mL) for 30 minutes. In some cases, platelets were incubated with pharmacologic inhibitors for 20 minutes at 37°C prior to adhesion. For superoxide anion measurement, platelets (1×10^8 platelets/mL) were incubated with dihydroethidium (DHE; 5 μmol/L) for 30 minutes, followed by nLDL/oxLDL (50 μg/mL) or $oxPC_{CD36}$/PAPC (5 μmol/L) for 15 minutes at 37°C, and lysate was prepared in methanol. DHE oxidation products present in the lysates were then analyzed by liquid chromatography mass spectrometry (LC-MS), with the specific superoxide reaction product (2-HE+) detected at an *m/z* ratio of 330.3 (see supplemental Method 3).

Evaluation of cGMP-PKG signaling

Intracellular cGMP was measured by enzyme immunoassay following the manufacturer's protocol. For measurement of PKG activity, washed platelets (7×10^8 platelets/mL) were stimulated with oxLDL or nLDL (50 μg/mL) for 15 minutes, lysed, and PKG immunoprecipitated. Immunoprecipitates were washed before incubation with 8-pCPT-cGMP (50 μmol/L) for 30 minutes in kinase buffer supplemented with adenosine triphosphate (ATP; 200 μmol/L). The supernatant was discarded following centrifugation. The pellets or recombinant PKG (300 ng) were added to a 96-well plate coated with recombinant PKG substrate and processed as directed by the manufacturers. In a second assay, constitutively active recombinant PKG1 (rPKG; 0.5 μg) was incubated with recombinant RhoA (rRhoA; 1 μg) in a reaction buffer (400 μmol/L ATP, 25 mmol/L 4-morpholinepropanesulfonic acid [pH 7.2], 12.5 mmol/L glycerol 2-phosphate, 25 mmol/L $MgCl_2$, 5 mmol/L EGTA, 2 mmol/L EDTA, and 0.25 mmol/L dithiothreitol) for 30 minutes at 37°C. The reaction was terminated by addition of ice-cold Laemmli buffer, and the proteins were separated by sodium dodecyl sulfate polyacrylamide gel electrophoresis (SDS-PAGE) and immunoblotted for RhoA or PKG1. In some cases, rPKG was incubated for 30 minutes with either xanthine (100 μmol/L)/xanthine oxidase (5 mU/mL) (X/XO) or potassium superoxide (KO_2; 1 mmol/L) prior to its addition to rRhoA.

Immunoprecipitation, immunoblotting, and cell fractionation

Immunoprecipitation, immunoblotting, and cell fractionation were performed as described in supplemental Methods 4.[26]

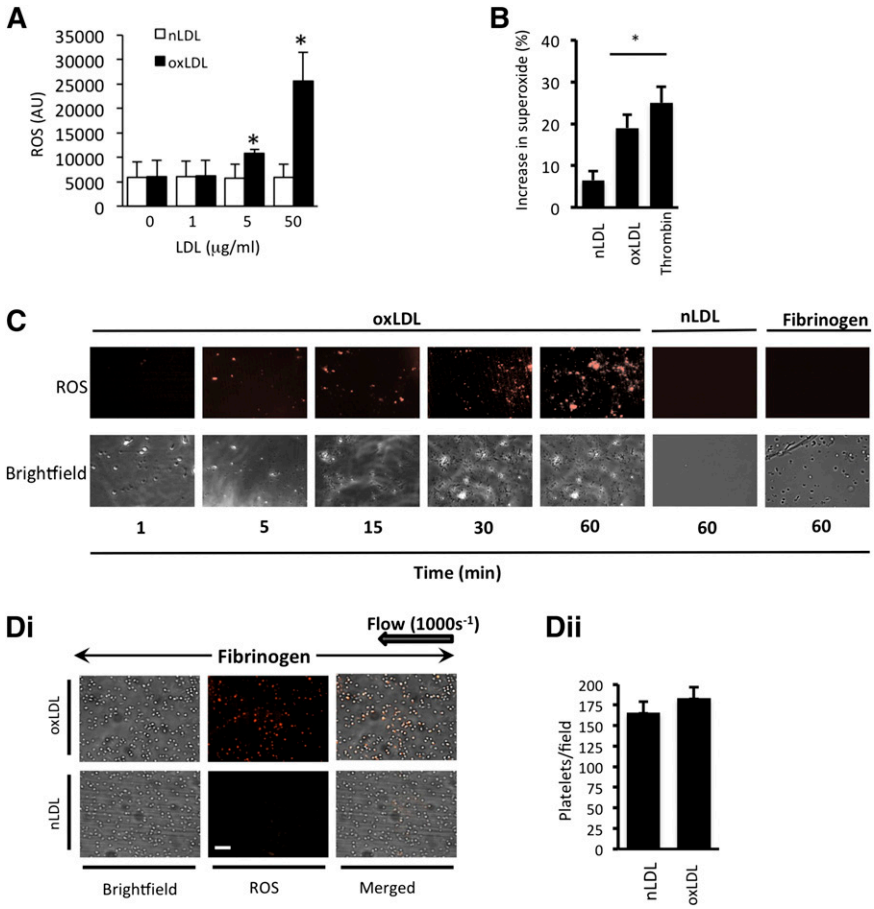

Figure 1. oxLDL stimulates ROS production in platelets. (A) Washed human platelets (1×10^8 platelets/mL) were incubated with the superoxide-detection probe for 30 minutes at 37°C and then treated with either nLDL or oxLDL (1-50 μg/mL) for 15 minutes, and fluorescence was measured at 650 nm (n = 4). *$P < .05$ compared with basal. (B) As in panel A, except platelets were incubated with DHE (5 μmol/L) for 30 minutes followed by LDL (50 μg/mL) or thrombin (0.01 U/mL) for 15 minutes, and DHE oxidation product for superoxide anion was measured by LC-MS. The data are presented as % increase in superoxide anion above basal (n = 4). *$P < .05$ compared with basal. (C) Washed human platelets (5×10^7 platelets/mL) were preincubated with a superoxide-detection probe for 30 minutes at 37°C and adhered to slides coated with oxLDL or nLDL (50 μg/mL) or human fibrinogen (100 μg/mL). Platelet fluorescence emission was then captured over time. Representative images of 5 separate experiments are shown. Scale bar, 20 μm. (D) Human platelets were stained with superoxide-detection probe, treated with nLDL or oxLDL (50 μg/mL), reconstituted with autologous RBCs, and perfused through fibrinogen-coated capillary tubes at arterial shear ($1000\ s^{-1}$). (i) Images were then captured under bright-field or fluorescence microscopy (n = 4 separate experiments with different blood donors). (ii) The number of platelets in each field is presented as mean ± SEM (n = 4).

Statistical analysis

Data are presented as means ± standard error of the mean (SEM). Differences between groups were calculated using the Student *t* test or analysis of variance and statistical significance taken at $P \leq .05$.

Results

oxLDL stimulates the generation of ROS in platelets

We first examined the ability of oxLDL to induce ROS generation. oxLDL (1-50 μg/mL), but not nLDL, caused a time- and concentration-dependent increase in ROS generation in suspended human platelets (Figure 1A and supplemental Figure 1A), which was diminished by preincubating platelets with the antioxidant *N*-acetylcysteine (100 μmol/L) and could not be detected in the absence of platelets (supplemental Figure 1B). Using a DHE assay linked to mass spectrometry, we found that superoxide anion was one of the ROS produced in response to oxLDL (Figure 1B). To visualize platelet-derived ROS, platelets were adhered to immobilized oxLDL under static conditions and observed using fluorescence microscopy. Platelets stained positively for ROS, with intracellular ROS observable after 5 minutes and continuing for up to 60 minutes (longest time tested) (Figure 1C). Platelets reconstituted with RBCs were then perfused over fibrinogen in the presence of oxLDL. Under these conditions, oxLDL, but not nLDL, stimulated ROS generation (Figure 1D). Control experiments confirmed that platelet preparations were free of leukocyte contamination (supplemental Figure 2) and that autofluorescence from the LDL or platelets did not account for the results (supplemental Figure 1C-D).

The stimulation of platelet ROS generation by oxLDL requires CD36 and NOX2

To investigate the role of CD36 as a potential receptor mediating ROS generation, we used three approaches: the nonantibody CD36 inhibitor SSO[27]; the oxidized phospholipid $oxPC_{CD36}$, a CD36-specific pathological ligand[28,29]; and murine platelets deficient in CD36. This strategy, particularly the use of $oxPC_{CD36}$, allowed us to account for any potential differences in sensitivity to human oxLDL between human and murine platelets. oxLDL-stimulated ROS generation in human platelets was abolished by SSO (100 μmol/L). Inhibition of alternate platelet scavenger receptors, SRA with fucoidan (Figure 2A) or LOX-1 with blocking antibodies (not shown), had no significant effect on oxLDL-stimulated ROS generation (Figure 2A). $OxPC_{CD36}$ (5 μmol/L) caused a level of ROS (Figure 2B) and superoxide anion generation (Figure 2C) in human platelets similar to that induced by oxLDL, while the control native lipid (PAPC) had no effect. To confirm the role of CD36 in mediating ROS generation, we used platelets from $CD36^{-/-}$ mice. Perfusion WT and CD36-deficient reconstituted blood over fibrinogen in the presence of $oxPC_{CD36}$ (5 μmol/L) led to ROS generation by WT, but not CD36-deficient, platelets (Figure 2Di). Similarly, $oxPC_{CD36}$ (5 μmol/L) stimulated ROS generation in suspended WT platelets, but not those deficient in CD36 (Figure 2E), confirming both the central role of CD36 and the specificity of $oxPC_{CD36}$ in activating this receptor.

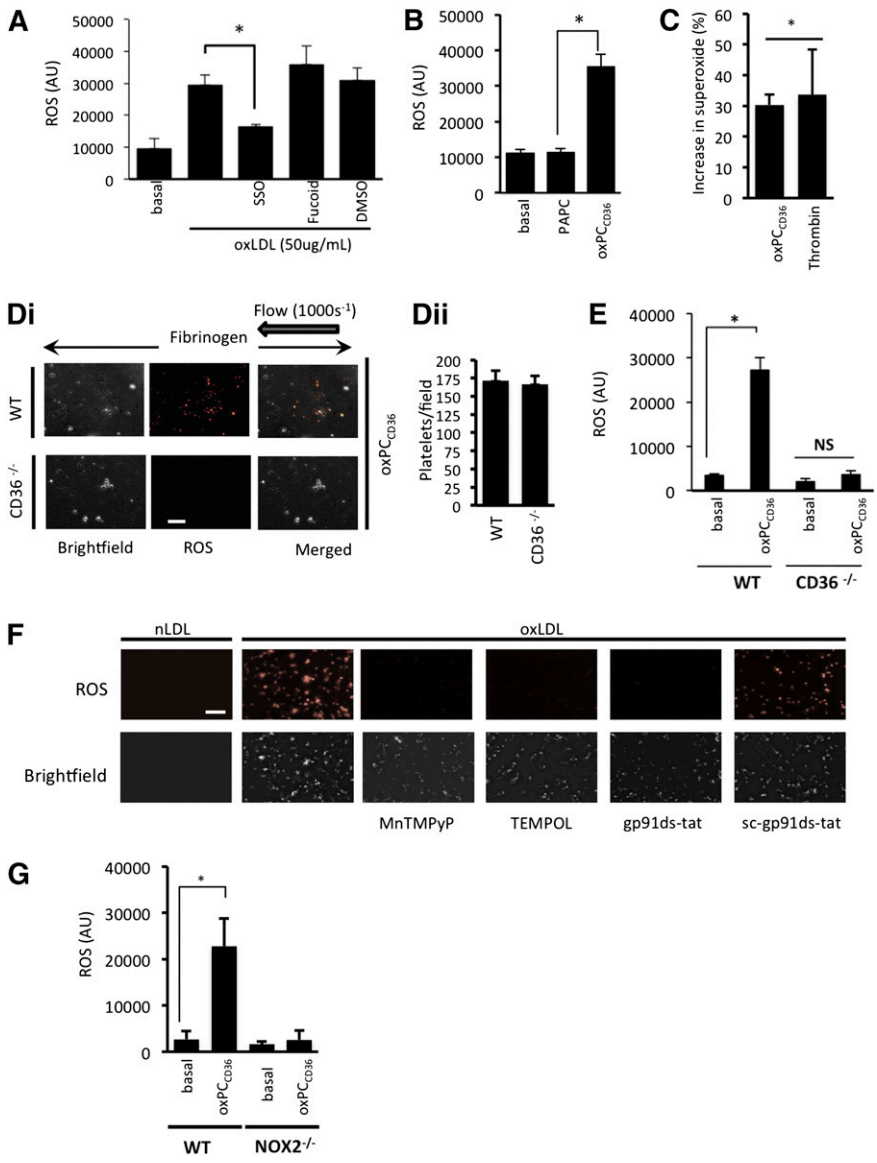

Figure 2. oxLDL stimulates platelet ROS production in a CD36- and NOX2-dependent manner. (A) Suspended human platelets (1×10^8 platelets/mL) were incubated with the superoxide-detection probe for 30 minutes at 37°C, then treated with oxLDL (50 μg/mL) for 15 minutes, in the presence or absence of SSO (100 μmol/L) or fucoidan (50 μg/mL). Fluorescence was measured at 650 nm (n = 4). $^*P < .05$ compared with oxLDL alone. (B) As in panel A, except platelets were treated with $oxPC_{CD36}$ or PAPC (5 μmol/L) ($^*P < .05$, PAPC compared with $oxPC_{CD36}$). (C) Suspended human platelets (1×10^8 platelets/mL) were incubated with DHE (5 μmol/L) for 30 minutes followed by $oxPC_{CD36}$ (5 μmol/L) or thrombin (0.1 U/mL) for 15 minutes, and the DHE oxidation product for superoxide anion was measured by LC-MS. The data are presented as % increase in superoxide above basal (n = 4). $^*P < .05$ compared with basal. (D) WT and $CD36^{-/-}$ murine platelets were stained with superoxide-detection probe and then treated with $oxPC_{CD36}$ (5 μmol/L). Reconstituted blood was perfused through fibrinogen-coated capillary tubes, and images of adherent platelets were then taken under bright-field or fluorescence microscopy (n = 4 separate experiments with different mice in each group). (i) Representative bright-field and fluorescence images are shown. (ii) The number of platelets in each field is presented as mean ± SEM (n = 4). (E) As in panel B, except WT and $CD36^{-/-}$ murine platelets were used (n = 4). $^*P < .05$, basal compared with $oxPC_{CD36}$. (F) Human platelets were treated with nLDL or oxLDL platelets in the presence of TEMPOL (1 mmol/L), MnTMPyP (100 μmol/L), gp91ds-tat, or sc-gp91ds-tat (2 μmol/L), or left untreated (control). Representative images of adherent platelets taken under bright-field or fluorescence microscopy are shown (n = 4). (G) Suspended murine platelets (1×10^8 platelets/mL), $NOX2^{-/-}$ or WT, were incubated with the superoxide-detection probe for 30 minutes at 37°C and then treated with $oxPC_{CD36}$ (5 μmol/L) for 15 minutes at 37°C, and fluorescence was measured at 650 nm (n = 4 individual mice). $^*P < .05$ compared with basal. NS, not significant.

We next addressed the source of platelet ROS. The fluorescence signal from adherent human platelets was ablated by the cell-permeable superoxide scavengers TEMPOL (1 mmol/L) and MnTMPyP (100 μmol/L) (Figure 2F), suggesting the presence of intracellular ROS. Pretreatment of platelets with the specific NOX2 inhibitor peptide gp91ds-tat,[30] but not its scrambled control sc-gp91ds-tat (both 2 μmol/L), prevented oxLDL stimulation of ROS (Figure 2F). Activation of $gp91^{phox}$/NOX2 represents a major source of intracellular platelet ROS. To confirm the link between CD36 and $gp91^{phox}$/NOX2, we used murine platelets deficient in NOX2. We observed that $oxPC_{CD36}$ increased ROS production in WT mice, but not $NOX2^{-/-}$ mice (Figure 2G). These data suggest that platelet NOX2 generates ROS downstream of CD36 in suspension and adhesion under both static and flow conditions.

NOX2 activation by oxLDL requires PKC-mediated phosphorylation of $p47^{phox}$

NOX2 activation requires PKC-mediated phosphorylation of cytosolic $p47^{phox}$ to drive its membrane association with $p22^{phox}$ and $gp91^{phox}$ and form the active holoenzyme.[31] Using an antibody that recognizes substrates phosphorylated on a PKC consensus sequence, we found that oxLDL, but not nLDL, caused phosphorylation of numerous PKC substrates with apparent molecular weights of 28, 47, 70, 88, and 110 kDa (Figure 3A). Similarly, $oxPC_{CD36}$ (5 μmol/L) caused phosphorylation of numerous PKC substrates in a CD36-dependent manner in murine platelets (supplemental Figure 3). Because PKC can be activated downstream of Src kinases,[32] we hypothesized that Src kinases constitutively associated with CD36 could sequentially activate PKC and NOX2. The inhibition of Src family kinases with PP2 ablated oxLDL-induced phosphorylation of PKC substrates (Figure 3A), consistent with the ability of oxLDL to induce CD36-dependent activation of Src-family kinase–dependent signaling (supplemental Figure 4).[10,19] We next examined the role of PKC in oxLDL-stimulated synthesis of ROS. Platelets adherent to immobilized oxLDL stained positive for ROS, which was abolished by inhibition of PKC with BIM-I (10 μmol/L), but not with its inactive analog BIM-V (Figure 3B). Using immunoprecipitation, we found that oxLDL stimulated phosphorylation of $p47^{phox}$, which was prevented when CD36 ligation was blocked or Src family kinases were inhibited (Figure 3C). The inhibition of PLC with U73122 or PKC with Ro31-8220 also blocked phospho-$p47^{phox}$. Furthermore, oxLDL, but not nLDL (50 μg/mL), induced relocation of

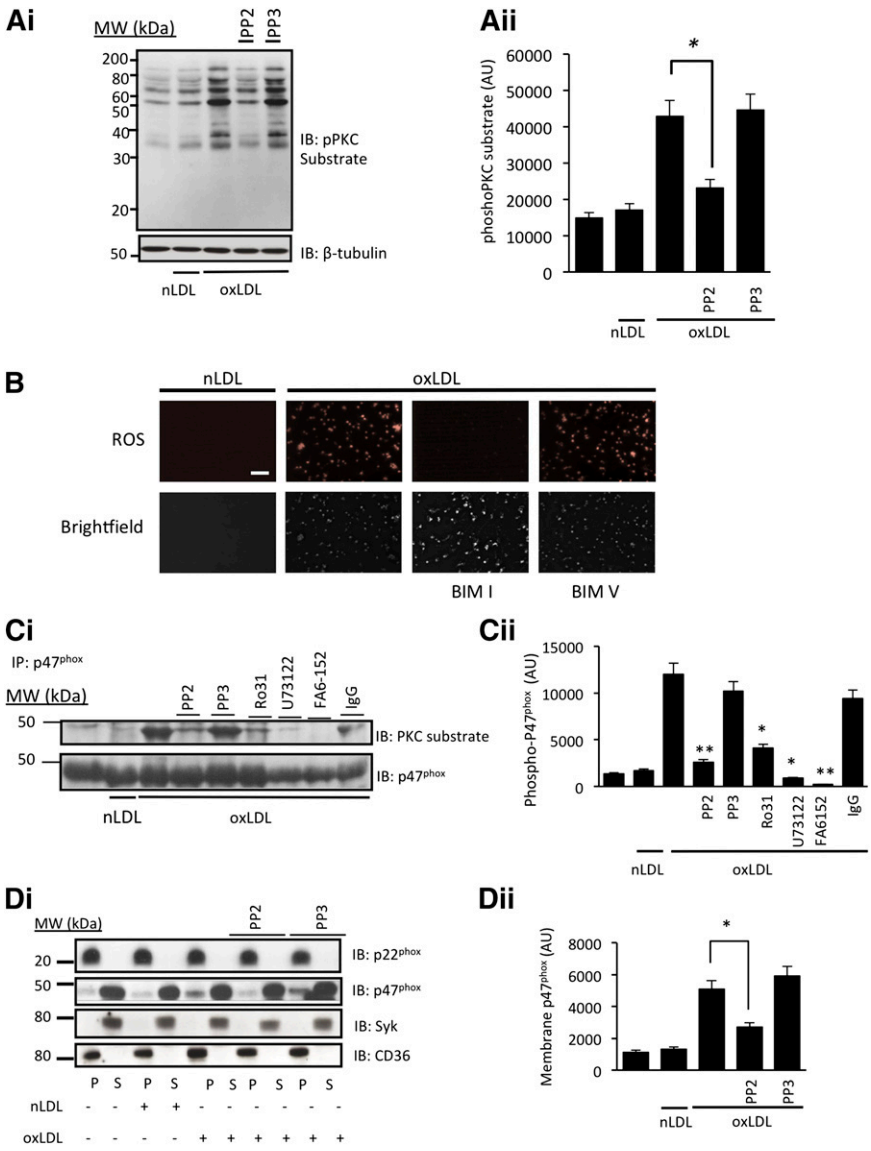

Figure 3. oxLDL-induced ROS generation and activation of gp91^{phox}/NOX2 requires PKC. (A) Washed human platelets incubated with apyrase, indomethacin, and EGTA were treated with PP2 and PP3 and then with LDL before being lysed with ice-cold lysis buffer.[26] Lysates were immunoblotted for phosphorylated PKC substrates. (i) Blots are representative of at least 3 experiments using different blood donors. (ii) Densitometric analysis of the blots. *$P < .05$ compared with oxLDL alone. (B) Washed human platelets (5×10^7 platelets/mL) were incubated with BIMI or BIMV (both 10 μmol/L) for 20 minutes at 37°C or left untreated (control) for 20 minutes at 37°C, incubated with a fluorescent superoxide detection probe for 30 minutes at 37°C, and adhered to slides coated with nLDL or oxLDL (50 μg/mL). Images are representative of 3 independent experiments with separate blood donors. Scale bar, 20 μm. (C) Washed human platelets were incubated with apyrase, indomethacin, and EGTA to prevent secondary signaling. In addition, they were also incubated with PP2/PP3 (20 μmol/L); U73122 (5 μmol/L); BIMI, BIMV, and Ro31-8220 (10 μmol/L); FA6-152; or a control IgG (both 5 μg/mL), then lysed with ice-cold lysis buffer.[26] p47^{phox} was then immunoprecipitated (IP) and immunoblotted (IB) using an antibody against phosphorylated PKC substrates. (i) Blots are representative of at least 3 experiments using different blood donors. (ii) Densitometric analysis of the blots. *$P < .05$, **$P < .01$ compared with oxLDL alone. (D) Washed human platelets were incubated with nLDL or oxLDL (50 μg/mL) for 15 minutes at 37°C, then diluted 1:1 with cell fractionation buffer (320 mmol/L sucrose, 4 mmol/L *N*-2-hydroxyethylpiperazine-*N*′-2-ethanesulfonic acid, and 0.5 mmol/L Na_3VO_4, protease inhibitor cocktail [pH 7.4]). The suspensions were immediately snap-frozen in liquid nitrogen and lysates separated into soluble (S) and particulate (P) fractions by ultracentrifugation. Proteins from each fraction were separated by SDS-PAGE and immunoblotted for p47^{phox}, p22^{phox}, CD36, and Syk. (i) Blots re representative of at least 3 experiments using different blood donors. (ii) Densitometric analysis of the blots. *$P < .05$ compared with oxLDL alone.

p47^{phox} from the cytosol to its counterpart, p22^{phox}, in the membrane (Figure 3D), which was blocked by the Src inhibitor PP2 (20 μmol/L) (Figure 3D). Together, these data suggest that oxLDL stimulates the phosphorylation and membrane recruitment of p47^{phox} by a CD36-tyrosine kinase-PKC–dependent pathway leading to the generation of ROS.

ROS increases platelet aggregation through the desensitization of cGMP-mediated platelet inhibition

Having established that oxLDL activated gp91^{phox}/NOX2 generation of ROS, we examined how this influenced platelet aggregation. oxLDL alone caused minor platelet aggregation and had no significant effect on the expression of major adhesion receptors (supplemental Figure 5A and Figure 6). Because cGMP signaling is known to regulate platelet function and TSP-1 inhibits platelet cGMP signaling independently of NO bioavailability through a CD36-dependent mechanism,[33] we assessed whether oxLDL influenced the inhibition of platelet aggregation by cGMP. The cell-permeable cGMP analog 8-pCPT-cGMP (50 μmol/L) inhibited thrombin-induced platelet aggregation (76.5% ± 11%). This inhibitory effect of cGMP was diminished in the presence of oxLDL (23.4% ± 15%; $P < .05$), but not nLDL (82% ± 16%) (Figure 4A). We observed similar effects when platelets were stimulated with collagen or ADP (supplemental Figure 5B-C) or when platelets were inhibited by NO (supplemental Figure 5D). In separate experiments, oxLDL reduced cGMP-mediated inhibition from 82% ± 8% to 26% ± 15% ($P < .05$) but was prevented if platelets were treated with by gp91ds-tat, where inhibition was similar to the absence of oxLDL (76% ± 7%; $P < .05$ compared with oxLDL alone) (Figure 4B). Consistent with the data from human platelets, treatment of WT platelets with $oxPC_{CD36}$ reduced sensitivity to inhibition by cGMP. In contrast sensitivity to inhibition by cGMP in the presence of $oxPC_{CD36}$ was maintained in NOX2$^{-/-}$ platelets (Figure 4C).

oxLDL-stimulated generation of ROS inhibits cGMP signaling

The reduced platelet sensitivity to 8-pCPT-cGMP suggested that oxLDL influenced either the availability of cGMP or its signaling through PKG, and so we explored these possibilities. Incubation of human platelets with 8-pCPT-cGMP (50 μmol/L) led to the rapid accumulation of intracellular cGMP, which was unaffected by nLDL/oxLDL (50 μg/mL) or $oxPC_{CD36}$/PAPC (5 μmol/L) (Figure 5A). In contrast, PKG

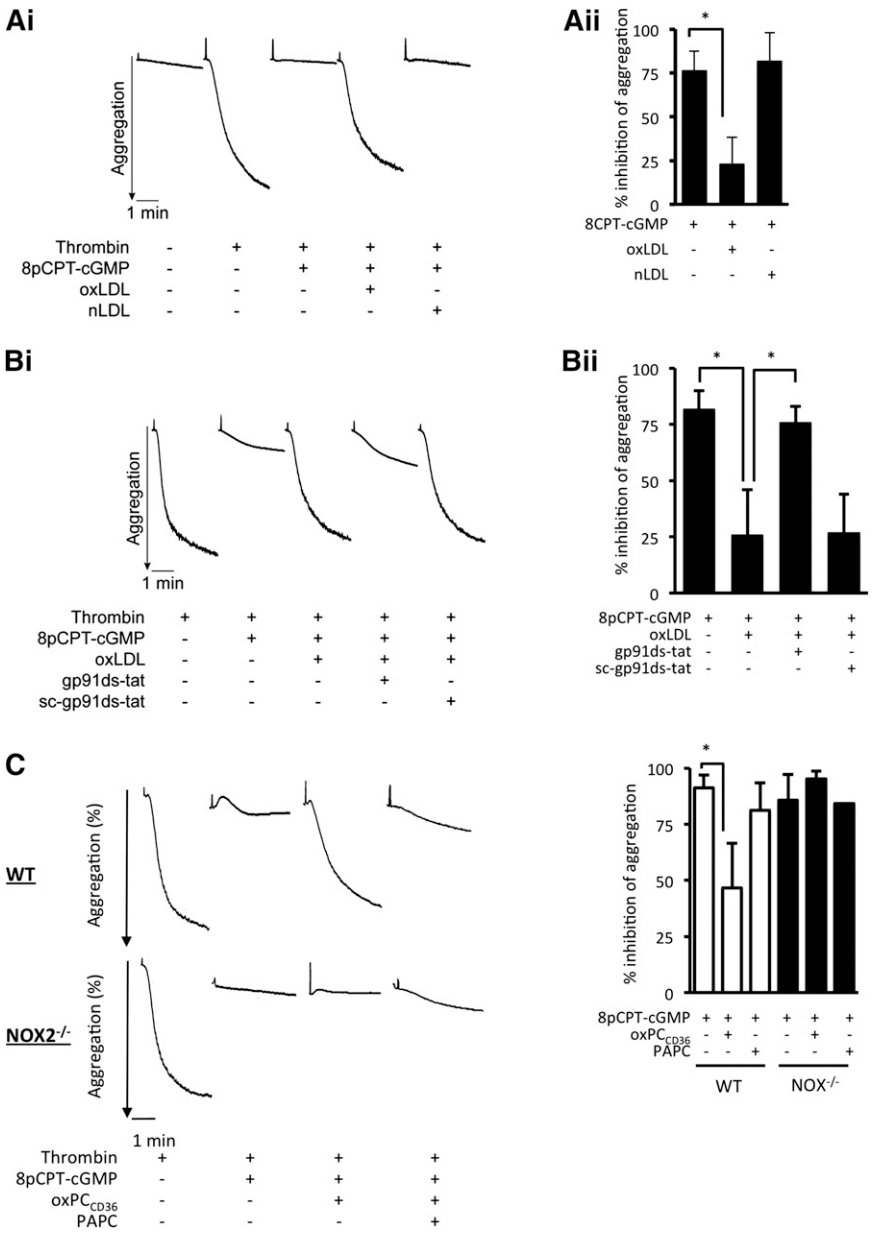

Figure 4. oxLDL modulates cGMP-mediated inhibition of platelet aggregation and arrest under conditions of flow. (A) Washed human platelets (3×10^8 platelets/mL) were incubated with 8-pCPT-cGMP (50 μmol/L) for 2 minutes alone or with nLDL or oxLDL (50 μg/ml) for 15 minutes followed by 8-pCPT-cGMP (50 μmol/L) for 2 minutes. Thrombin-stimulated aggregation was then measured under constant stirring (1000 rpm) at 37°C for 3 minutes. Aggregation was recorded for 3 minutes. (i) Representative aggregation traces. (ii) Percent inhibition of thrombin induced aggregation by cGMP is presented as mean ± SD (n = 4, $^*P < .05$ compared with absence of oxLDL). (B) As in panel A, except platelets were incubated with gp91ds-tat or its scrambled control (both 2 μmol/L) prior to the addition of oxLDL. (i) Representative aggregation traces. (ii) Percent inhibition of thrombin induced aggregation by cGMP is presented as mean ± SD (n = 4). $^*P < .05$. (C) As in panel A, except WT and NOX2$^{-/-}$ murine platelets were treated with $oxPC_{CD36}$ or PAPC (5 μmol/L) for 15 minutes followed by 8-pCPT-cGMP (50 μmol/L) for 2 minutes. (i) Representative aggregation traces are shown. (ii) Percent inhibition of thrombin induced aggregation by cGMP is presented as mean ± SD (n = 3). $^*P < .05$ compared with the absence of $oxPC_{CD36}$.

immunoprecipitated from oxLDL-treated platelets showed diminished sensitivity to exogenous cGMP, whereas PKG activity from nLDL-treated platelets remained at control (cGMP-stimulated) levels (Figure 5B). In order to explore whether the ROS affected PKG activity, we next used an in vitro kinase assay with RhoA as a target for cGMP/PKG signaling.[34] We reasoned that if intracellular ROS modulated PKG activity, then exposure of PKG to oxidative stress in vitro could reduce its capacity to phosphorylate a target protein. Incubation of rRhoA with constitutively active rPKG induced phosphorylation of rRhoA on serine^{188}. No phosphorylation was observed in the absence of ATP or rPKG1. Pretreatment of rPKG1 with distinct generators of superoxide, xanthine (10 μmol/L)/xanthine oxidase (5 mU/mL) or potassium superoxide (1 mmol/L), ablated its ability to phosphorylate rRhoA (Figure 5C).

Having found that PKG activity was compromised by oxLDL, we determined how downstream signaling was affected by measuring the phosphorylation of vasodilator-activated phosphoprotein (VASP) at serine^{239} (ser^{239}), a marker of PKG activity.[35] Treatment of platelets with 8-pCPT-cGMP (50 μmol/L) induced a robust phosphorylation of VASP-ser^{239}, which was prevented by oxLDL (Figure 5D-F). This confirmed that oxLDL inhibited cGMP signaling independently of any effects on NO bioavailability or cGMP synthesis. Blocking platelet CD36 receptors with FA6-152 (5 μg/mL) (Figure 5D) and inhibiting Src kinases with PP2 (20 μmol/L) (Figure 5E) and PKC with Ro31-8220 (10 μmol/L) or BIM-I (10 μmol/L) (Figure 5F) prevented the ability of oxLDL to block the phosphorylation of VASP-ser^{239} induced by 8-pCPT-cGMP (50 μmol/L). We next confirmed the role of ROS in oxLDL-mediated regulation of cGMP signaling. The ability of oxLDL to modulate cGMP signaling was prevented by pretreatment of platelets with TEMPOL (1 mmol/L) and MnTMPyP (100 μmol/L) (Figure 6A) and gp91ds-tat, but not scr-gp91ds-tat (2 μmol/L) (Figure 6B). Consistent with these data, we found that 8-pCPT-cGMP (50 μmol/L) stimulated VASP-ser^{239} phosphorylation in both WT and NOX2$^{-/-}$ murine platelets but that the presence of $oxPC_{CD36}$ blocked phospho–VASP-ser^{239} in WT, but not NOX2$^{-/-}$, mice (Figure 6Ci), with similar effects observed with oxLDL (supplemental Figure 7A). Here,

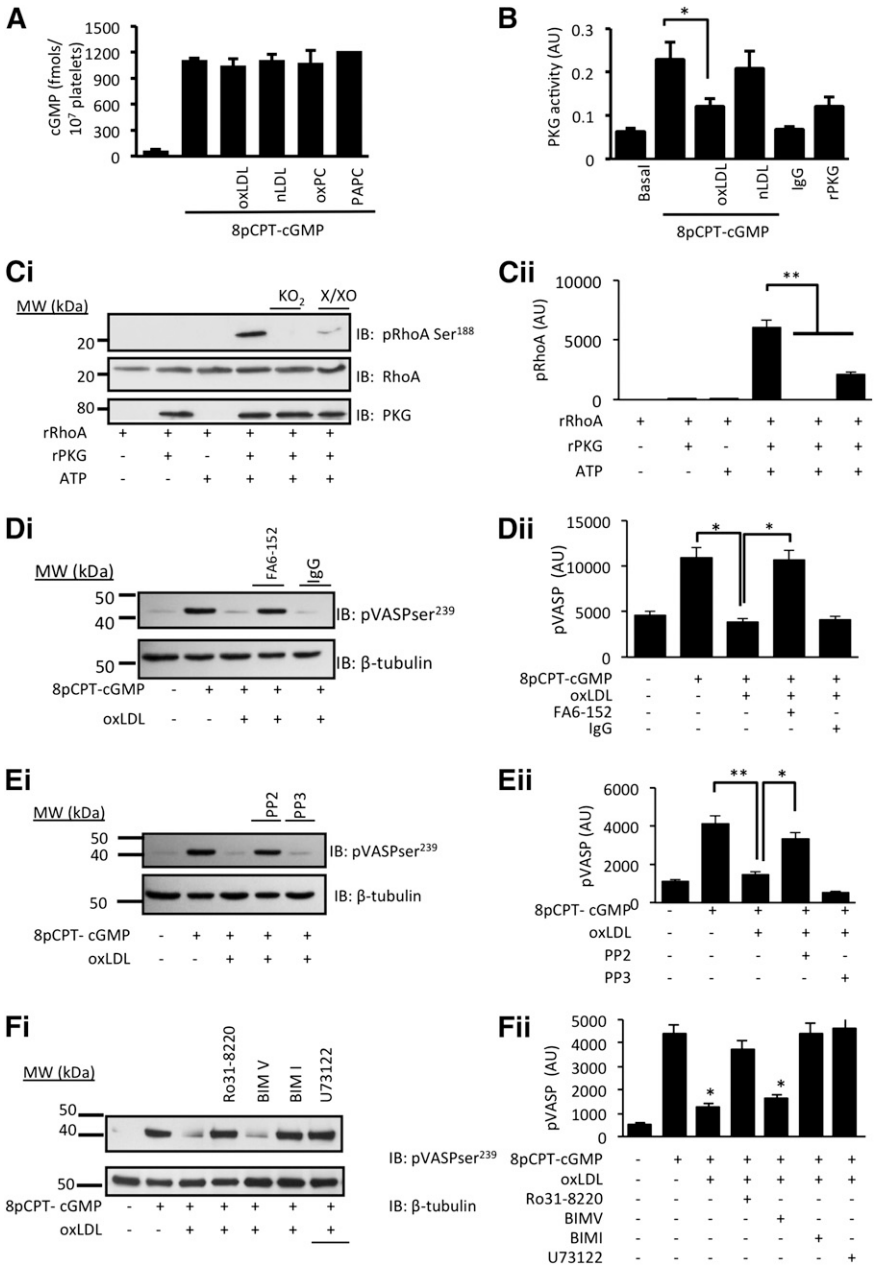

Figure 5. oxLDL inhibits cGMP signaling through a mechanism that requires CD36, Src kinases, and PKC. (A) Human platelets (3×10^8 platelets/mL) were incubated with nLDL (50 μg/mL), oxLDL (50 μg/ml), $oxPC_{CD36}$ (5 μmol/L), or PAPC (5 μmol/L) prior to the addition of 8-pCPT-cGMP (50 μmol/L) for 2 minutes. Platelets were washed and lysed, and intracellular cGMP concentrations were measured by enzyme immunoassay (n = 4). (B) Human platelets (5×10^8 platelets/mL) were treated with nLDL or oxLDL (50 μg/mL) for 15 minutes, lysed, and PKG1 immunoprecipitated. Immunoprecipitates were incubated with exogenous cGMP and PKG activity measured spectrophotometrically at 450 nm. $^*P < .05$ compared with the absence of oxLDL. (C) In an in vitro kinase assay, constitutively active rPKG (0.5 μg) was incubated with rRhoA (1 μg) for 30 minutes at 37°C. In some cases, rPKG was preincubated for 30 minutes with either xanthine (100 μmol/L)/xanthine oxidase (5 mU/mL) (X/XO) or KO_2 (1 mmol/L) before addition to rRhoA. Phosphorylation was terminated by Laemmli buffer, the mixture separated by SDS-PAGE and immunoblotted for phosphoRhoA-Ser^{188}, total RhoA, or PKG1. $^{**}P < .01$ for rPKG alone compared with the presence of X/XO or KO_2. (D) Washed human platelets (5×10^8 platelets/mL) preincubated with apyrase (2 U/mL), indomethacin (10 μmol/L), and EGTA (1 mmol/L) were treated with oxLDL (50 μg/mL) in the presence or absence of the CD36 blocking antibody FA6-152 or IgG (5 μg/mL) prior to the addition of 8-pCPT-cGMP (50 μmol/L) for 2 minutes. Platelets were lysed, separated by SDS-PAGE, and immunoblotted (IB) for phospho–VASP-ser^{239} and β-tubulin. $^*P < .05$ compared with the absence of oxLDL and oxLDL in the presence and absence of FA6. (E) As in panel D, except platelets were treated with PP2 or PP3. $^*P < .05$ compared with the absence of oxLDL and oxLDL in the presence and absence of PP2). (F) As in panel D, except platelets were treated with Ro31-8220, BIMI, BIMV, U73122, or BAPTA-AM prior to the addition of oxLDL (50 μg/mL) for 15 minutes and 8-pCPT-cGMP (50 μmol/L) for 2 minutes. In all figures, subpanel i shows blots representative of at least 3 experiments using different blood donors, and subpanel ii shows densitometric analysis of the blots. $^*P < .05$ compared with oxLDL alone.

phospho-VASP appears as a doublet, which occurs with incomplete dual phosphorylation (phospho-$VASP^{157/239}$), suggesting that murine platelets may be less sensitive to cGMP signaling than human platelets. Importantly, oxLDL-induced tyrosine phosphorylation was unaffected in $NOX2^{-/-}$ mice (supplemental Figure 7B).

oxLDL and hyperlipidemia decrease platelet sensitivity to cGMP through NOX2

Finally, the physiological implications of our findings for platelet function were addressed. Under arterial shear (1000 s^{-1}), immobilized fibrinogen supported platelet deposition and thrombus formation leading to surface coverage of 10.9% ± 2.9% (supplemental Video 1), which was unaffected by LDL (supplemental Figure 8A). In contrast, 8pCPT-cGMP (50 μmol/L) reduced surface coverage to 4.1% ± 3.1% ($P \leq .05$) (Figure 7A; supplemental Video 2). Consistent with the aggregation data, the presence of oxLDL blocked cGMP-mediated inhibition, with surface coverage remaining at 10.3% ± 1.8% ($P \leq .05$) (supplemental Video 3). Incubation of platelets with TEMPOL (1 mmol/L), MnTMPyP (100 μmol/L), and gp91ds-tat (2 μM) led to platelet surface coverage values of 5.4% ± 1.6% ($P \leq .05$), 3.7% ± 1.0% ($P \leq .05$), and 4.8% ± 2.7% ($P \leq .05$), respectively, indicating that oxLDL cannot influence cGMP-mediated platelet inhibition in the absence of ROS generation (Figure 7A; supplemental Videos 4-6). Similar data were produced when we used collagen as the adhesive surface (supplemental Figure 8B).

To examine if NOX2 had a role in platelet hyperactivity associated with hyperlipidemia, we examined the sensitivity of platelets from hyperlipidemic $ApoE^{-/-}$ mice, which had been infused with gp91ds-tat or the scrambled control, to the inhibitory effects of 8-pCPT-cGMP. Platelet function was evaluated directly by flow cytometry in whole blood ex vivo to avoid any confounding effects on the vessel wall.[36] In WT mice, 8-pCPT-cGMP (50 μmol/L) caused robust inhibition of ADP (10 μmol/L)-induced fibrinogen binding (81.4% ± 4%)

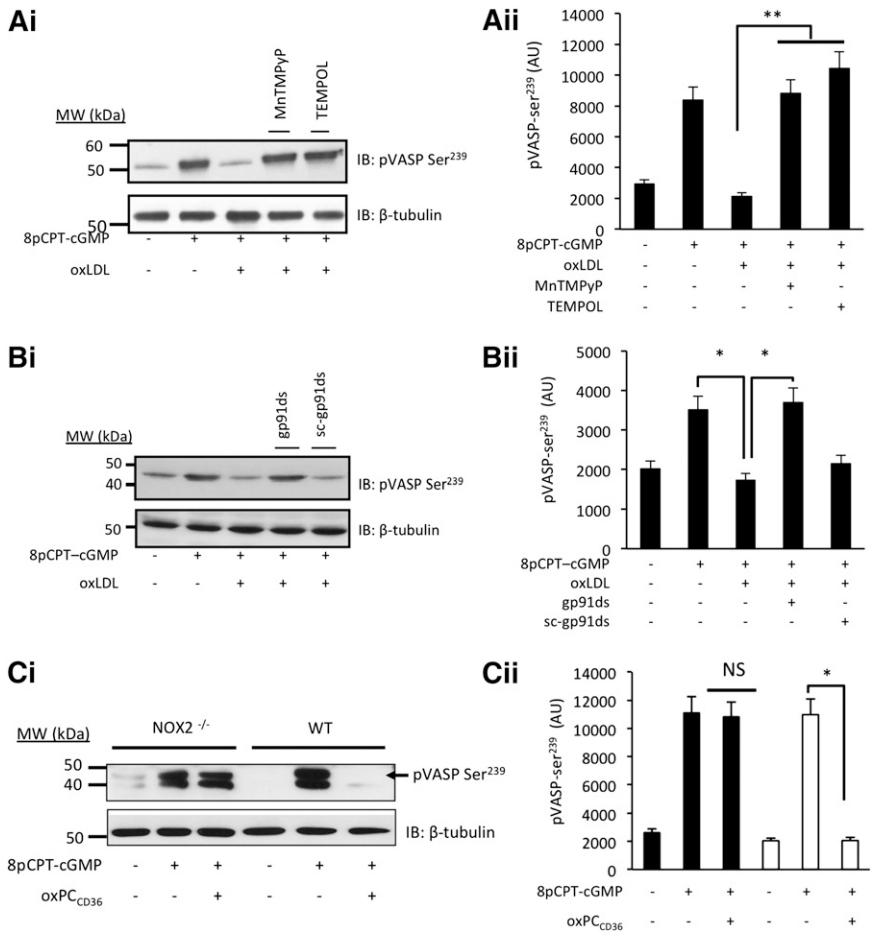

Figure 6. oxLDL inhibits cGMP-signaling through a mechanism that requires NOX2 and intracellular ROS. (A) Platelets (5×10^8 platelets/mL) were incubated with apyrase (2 U/mL), indomethacin (10 μmol/L), and EGTA (1 mmol/L) and treated with MnTMPyP (100 μmol/L) or TEMPOL (1 mmol/L) prior to the addition of 8-pCPT-cGMP (50 μmol/L) for 2 minutes. Platelets were lysed, separated by SDS-PAGE, and immunoblotted (IB) for phospho–VASP-ser^{239}. (i) Blots are representative of at least 3 experiments using different blood donors. (ii) Densitometric analysis of the blots. $^{**}P < .01$ compared with the absence of inhibitors. (B) As in panel A, except that in some cases, platelets were pretreated with gp91ds-tat or its scrambled control (both 2 μmol/L). Blots are representative of at least 3 separate experiments. $^{*}P < .05$ for CGMP alone, cGMP/oxLDL, and oxLDL in the presence and absence of gp91da-tat. (C) As in panel A, except NOX2-deficient or WT murine platelets were treated with 8pCPT-cGMP (50 μmol/L) and $oxPC_{CD36}$ (5 μmol/L). $^{*}P < .05$ compared with the absence of $oxPC_{CD36}$. NS, not significant.

(Figure 7Bi-ii), which was severely compromised in hyperlipidemic ApoE$^{-/-}$ mice infused with the control peptide (46.6% ± 12%; $P < .05$) (Figure 7Bi,iii). Importantly, this cGMP hyporesponsive phenotype was corrected by the infusion of gp91ds-tat (10 mg/kg per day), where the ability of cGMP to inhibit fibrinogen binding was the same as WT (76.1% ± 5.7%) (Figure 7Biv).

Discussion

Numerous studies have now pinpointed CD36 as a receptor that drives multiple aspects of platelet function in response to a variety of mediators. Plasma- and platelet-derived TSP-1 contributes to physiological platelet adhesion and platelet endothelial crosstalk.[33,37] In contrast, endothelial-derived microparticles, advanced glycation end products, and MRP14 can drive thrombosis.[38-40] Platelet hyperactivity that underpins arterial thrombosis in the context of dyslipidemia is thought to proceed through the actions of oxLDL.[10,11,41] However, whereas the activation of platelets by different forms of oxLDL has been widely reported and occurs through a variety of mechanisms, it has been difficult to understand how oxLDL may act in vivo given its modest effects on platelet activation in vitro and ex vivo.[7,8,16,42,43] With this in mind, we set out to explore how oxLDL drives platelet activation independently of other agonists. The data reported here (1) demonstrate that oxLDL ligation of platelet CD36 increases platelet ROS and superoxide generation through NOX2, (2) describe the components of a CD36-linked signaling pathway that activates NOX2, and (3) highlight a mechanism by which CD36-stimulated ROS generation can drive platelet hyperactivity examined both in vitro and ex vivo. Although earlier studies have suggested that modified LDL can increase ROS generation in suspended platelets, the physiological significance of this has remained unclear.[44] We demonstrate that both adherent platelets and platelets in flowing whole blood produced sustained generation of ROS in response to oxLDL. The use of cell-permeable superoxide scavengers demonstrated that the ROS produced were primarily intracellular and were both prevented by the NOX2-specific inhibitor gp91ds-tat and ablated in murine platelets deficient in NOX2. Examination of the molecular mechanisms underpinning ROS generation showed that ligation of CD36 was essential, because the effects of oxLDL could be reproduced by a CD36-specific ligand, was blocked by CD36 inhibitors, and was absent in CD36-deficient murine platelets. Therefore, consistent with studies in smooth muscle, oxLDL stimulates ROS generation through CD36-dependent activation of NOX2.[20] Recently, we have shown that ligation of CD36 by oxLDL caused the sequential activation of Src kinases, Syk and PLCγ2,[19] and here show that this extends to the activation of PKC and NOX2. The activation of PKC in response to oxLDL led to the phosphorylation and membrane compartmentalization of p47^{phox}, a necessary step in the formation of the active NOX2 complex,[31] in a CD36- and Src-family kinase–dependent manner. The use of 2 structurally distinct PKC inhibitors, Ro31-8220 and BIM-I, blocked both phosphorylation of p47^{phox} and ROS generation. Together, these data suggest that CD36-stimulated ROS generation in response to oxLDL involves a CD36, Src-family kinase, PKC, and NOX2 pathway (Figure 7C), although the precise roles of Syk and PLCγ2 require more detailed investigation.

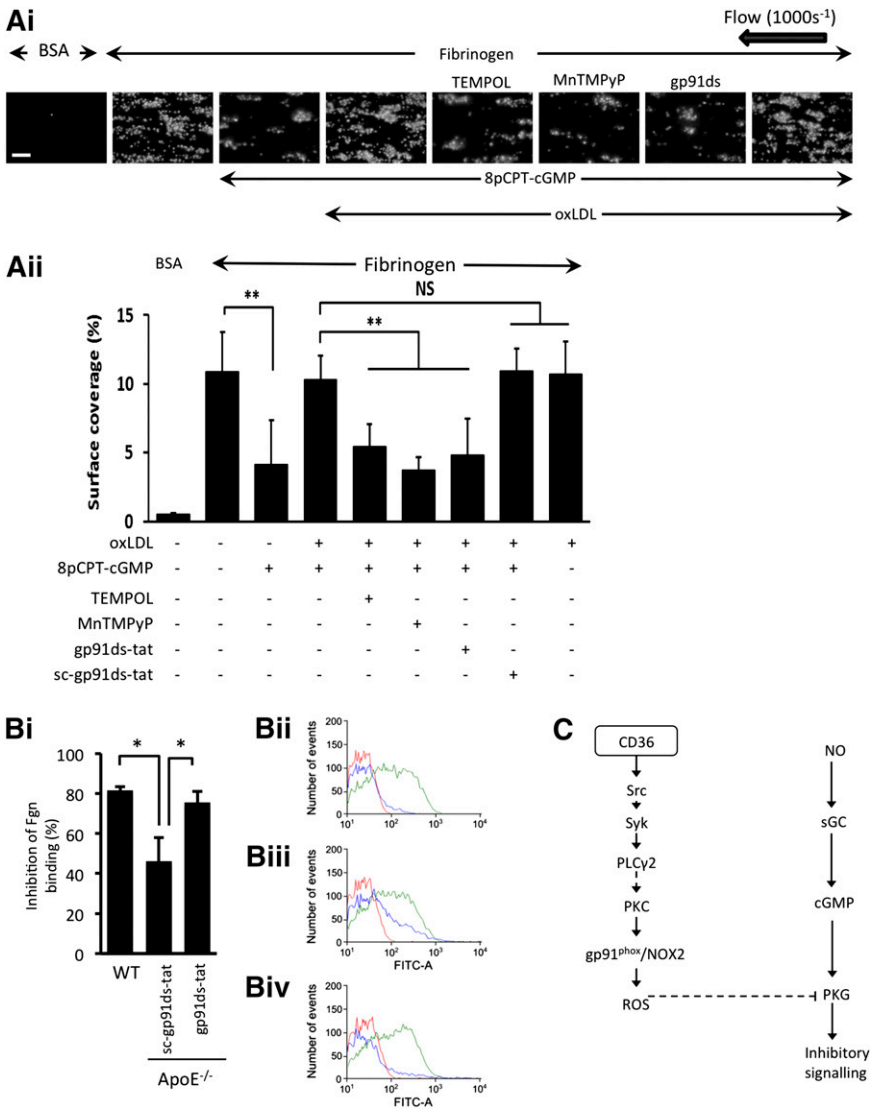

Figure 7. oxLDL and hyperlipidemia caused decreased platelet sensitivity to cGMP through NOX2. (A) Human platelets were stained with $DiOC_6$ (1 μmol/L) for 10 minutes at 37°C, reconstituted with RBCs, treated with either nLDL or oxLDL for 15 minutes, and then perfused through fibrinogen (1 mg/mL) or bovine serum albumin (BSA)-coated capillary tubes for 2 minutes at a shear rate of 1000 s^{-1}. (i) Shown are images representative of 3 independent experiments with separate blood donors. Scale bar, 20 μm. (ii) Data are presented as surface area coverage (%) (n = 3). $^{**}P < .01$, fibrinogen compared with cGMP, and oxLDL in the presence and absence of inhibitors. (B) Blood from WT and $ApoE^{-/-}$ mice were stimulated with ADP (10 μM) in the presence and absence of 8pCPT-cGMP (50 μmol/L) and platelet fibrinogen binding measured by flow cytometry. (i) Data are presented as % inhibition of fibrinogen (Fgn) binding and are expressed as mean ± SEM taken from 9 individual mice for each group. $^{*}P < .05$. Representative fluorescence-activated cell sorter histograms of fibrinogen binding for WT (ii), sc-gp91ds-tat (iii), and gp91ds-tat (iv). Each histogram shows fibrinogen binding at basal (red line), ADP (10 μM) (green line), and 8pCPT-cGMP (50 μmol/L)/ADP (blue line). (C) Summary of the proposed signaling pathway downstream of CD36 through which oxLDL activates $gp91^{phox}$/NOX2 and suppresses PKG signaling. sGC, soluble guanylyl cyclase; NS, not significant.

In murine models of hyperlipidemia, platelet CD36 plays a key role in propagating platelet activation and thrombosis,[11] whereas in humans, increased platelet CD36 receptor expression correlates with elevated oxLDL-mediated platelet activity and thrombotic risk.[17] Therefore, we were initially surprised to find that oxLDL caused only minor platelet aggregation and failed to influence accrual under flow (supplemental Figures 5A and 8A). However, these observations are consistent with many studies that show oxLDL alone induces only minor platelet activation but potentiates the effects of other agonists,[6-8,10,42] and they suggest that oxLDLs influence platelet function through mechanisms beyond direct activation. The NO/cGMP/PKG signaling pathway is critical to the control of platelet function in vivo,[45] and our finding that oxLDL causes a profound desensitization of cGMP signaling in platelets shows a new mechanism by which oxidized lipids may promote platelet hyperactivity. Treatment of platelets with oxLDL blocked the ability of cGMP to inhibit platelet function. The molecular mechanisms underpinning these observations suggest that oxLDL reduced PKG sensitivity to cGMP activation, which in turn prevented downstream signaling. This dampening of cGMP signaling through the generation of intracellular NOX2-derived ROS is therefore independent of reduced NO bioavailability through consumption by extracellular ROS.[46] Because $NOX2^{-/-}$ platelets retain sensitivity to cGMP inhibition in the presence of oxLDL, we suggest that NOX2 is a potentially critical component involved in the oxLDL-mediated platelet thrombosis. We support this with observations that platelets from hyperlipidemic mice show a reduced sensitivity to cGMP when tested ex vivo. Critically, platelet hyporesponsiveness to cGMP is corrected by long-term infusion of gp91ds-tat into these mice, suggesting that platelet NOX2 may be a target for controlling platelet hyperactivity. Our observations are consistent with studies demonstrating that NOX2 influences platelet recruitment into growing thrombi in mice[21] and with the observation that platelets from subjects with chronic granulomatous disease, who are deficient in NOX2, have reduced platelet activity.[47] Importantly, our data chime with clinical studies that observed impaired responsiveness to NO and cGMP ex vivo in subjects in whom the disease is associated with platelet hyperactivity.[13-15]

In the complex conditions found in vivo, the balance between pro- and antiplatelet factors determines platelet function. Platelets from patients with dyslipidemia have recently been shown to bind oxLDL in circulation, which is associated with increased platelet activation, through unknown mechanisms.[48] Because CD36 is competent to bind its ligands in the absence of platelet activation, our data could suggest that in patients with dyslipidemia, a subset of platelets are bound to oxLDL and potentially insensitive to the inhibitory effects of cGMP signaling. This could reduce the threshold for platelet activation as sites of vascular injury and suggest that a prothrombotic phenotype may be

caused, at least in part, through the modulation of platelet sensitivity to cyclic nucleotide signaling rather than direct activation. We conclude that oxLDL can use a redox-dependent mechanism to induce crosstalk between CD36 and cyclic nucleotide signaling pathways, which may promote unwanted platelet activation.

Acknowledgments

The authors thank Ben Spurgeon and Robert Law for assisting with processing the figures.

This study was funded by grants from the British Heart Foundation (PG/11/37/28884 and PG/13/90/30578) and Heart Research UK (RG2614).

Authorship

Contribution: S.M. designed the research, performed experiments, analyzed data, and wrote the manuscript; C.W., K.S.W., A.A., C.M., Z.R., and H.J. performed experiments; S.W. designed the research and provided essential materials; N.Y. performed experiments; M.F. provided essential materials; M.K. designed the research and provided essential materials; and K.M.N. designed the research, analyzed data, and wrote the manuscript.

Conflict-of-interest disclosure: The authors declare no competing financial interests.

Correspondence: Khalid M. Naseem, Thrombosis Research Laboratory (013/014), Hardy Building, University of Hull, Cottingham Road, Hull HU6 7RX, UK; e-mail: khalid.naseem@hyms.ac.uk.

References

1. Schmidt HH, Lohmann SM, Walter U. The nitric oxide and cGMP signal transduction system: regulation and mechanism of action. *Biochim Biophys Acta.* 1993;1178(2):153-175.
2. Carvalho AC, Colman RW, Lees RS. Platelet function in hyperlipoproteinemia. *N Engl J Med.* 1974;290(8):434-438.
3. Davì G, Romano M, Mezzetti A, et al. Increased levels of soluble P-selectin in hypercholesterolemic patients. *Circulation.* 1998; 97(10):953-957.
4. Pawlowska Z, Swiatkowska M, Krzeslowska J, Pawlicki L, Cierniewski CS. Increased platelet-fibrinogen interaction in patients with hypercholesterolemia and hypertriglyceridemia. *Atherosclerosis.* 1993;103(1):13-20.
5. Colas R, Sassolas A, Guichardant M, et al. LDL from obese patients with the metabolic syndrome show increased lipid peroxidation and activate platelets. *Diabetologia.* 2011;54(11):2931-2940.
6. Ardlie NG, Selley ML, Simons LA. Platelet activation by oxidatively modified low density lipoproteins. *Atherosclerosis.* 1989;76(2-3): 117-124.
7. Naseem KM, Goodall AH, Bruckdorfer KR. Differential effects of native and oxidatively modified low-density lipoproteins on platelet function. *Platelets.* 1997;8(2-3):163-173.
8. Hackeng CM, Huigsloot M, Pladet MW, Nieuwenhuis HK, van Rijn HJ, Akkerman JW. Low-density lipoprotein enhances platelet secretion via integrin-alphaIIbbeta3-mediated signaling. *Arterioscler Thromb Vasc Biol.* 1999; 19(2):239-247.
9. Keidar S, Aviram M, Grenadier E, Markiewicz W, Brook JG. Low-density lipoprotein derived from atherosclerotic patients enhances macrophage cholesterol accumulation and in vitro platelet aggregation. *Biochem Med Metab Biol.* 1989; 41(2):117-124.
10. Chen K, Febbraio M, Li W, Silverstein RL. A specific CD36-dependent signaling pathway is required for platelet activation by oxidized low-density lipoprotein. *Circ Res.* 2008;102(12): 1512-1519.
11. Podrez EA, Byzova TV, Febbraio M, et al. Platelet CD36 links hyperlipidemia, oxidant stress and a prothrombotic phenotype. *Nat Med.* 2007;13(9): 1086-1095.
12. Korporaal SJ, Van Eck M, Adelmeijer J, et al. Platelet activation by oxidized low density lipoprotein is mediated by CD36 and scavenger receptor-A. *Arterioscler Thromb Vasc Biol.* 2007; 27(11):2476-2483.
13. Willoughby SR, Stewart S, Holmes AS, Chirkov YY, Horowitz JD. Platelet nitric oxide responsiveness: a novel prognostic marker in acute coronary syndromes. *Arterioscler Thromb Vasc Biol.* 2005;25(12):2661-2666.
14. Riba R, Nicolaou A, Troxler M, Homer-Vaniasinkam S, Naseem KM. Altered platelet reactivity in peripheral vascular disease complicated with elevated plasma homocysteine levels. *Atherosclerosis.* 2004;175(1):69-75.
15. Russo I, Traversa M, Bonomo K, et al. In central obesity, weight loss restores platelet sensitivity to nitric oxide and prostacyclin. *Obesity (Silver Spring).* 2010;18(4):788-797.
16. Maschberger P, Bauer M, Baumann-Siemons J, et al. Mildly oxidized low density lipoprotein rapidly stimulates via activation of the lysophosphatidic acid receptor Src family and Syk tyrosine kinases and Ca2+ influx in human platelets. *J Biol Chem.* 2000;275(25):19159-19166.
17. Ghosh A, Murugesan G, Chen K, et al. Platelet CD36 surface expression levels affect functional responses to oxidized LDL and are associated with inheritance of specific genetic polymorphisms. *Blood.* 2011;117(23):6355-6366.
18. Nergiz-Unal R, Lamers MME, Van Kruchten R, et al. Signaling role of CD36 in platelet activation and thrombus formation on immobilized thrombospondin or oxidized low-density lipoprotein. *J Thromb Haemost.* 2011;9(9): 1835-1846.
19. Wraith KS, Magwenzi S, Aburima A, Wen Y, Leake D, Naseem KM. Oxidized low-density lipoproteins induce rapid platelet activation and shape change through tyrosine kinase and Rho kinase-signaling pathways. *Blood.* 2013;122(4):580-589.
20. Li W, Febbraio M, Reddy SP, Yu D-Y, Yamamoto M, Silverstein RL. CD36 participates in a signaling pathway that regulates ROS formation in murine VSMCs. *J Clin Invest.* 2010;120(11):3996-4006.
21. Krötz F, Sohn HY, Gloe T, et al. NAD(P)H oxidase-dependent platelet superoxide anion release increases platelet recruitment. *Blood.* 2002;100(3):917-924.
22. Roberts W, Magwenzi S, Aburima A, Naseem KM. Thrombospondin-1 induces platelet activation through CD36-dependent inhibition of the cAMP/protein kinase A signaling cascade. *Blood.* 2010;116(20):4297-4306.
23. Gerry AB, Satchell L, Leake DS. A novel method for production of lipid hydroperoxide- or oxysterol-rich low-density lipoprotein. *Atherosclerosis.* 2008;197(2):579-587.
24. el-Saadani M, Esterbauer H, el-Sayed M, Goher M, Nassar AY, Jürgens G. A spectrophotometric assay for lipid peroxides in serum lipoproteins using a commercially available reagent. *J Lipid Res.* 1989;30(4):627-630.
25. Magwenzi SG, Ajjan RA, Standeven KF, Parapia LA, Naseem KM. Factor XIII supports platelet activation and enhances thrombus formation by matrix proteins under flow conditions. *J Thromb Haemost.* 2011;9(4):820-833.
26. Aburima A, Wraith KS, Raslan Z, et al. cAMP signaling regulates platelet myosin light chain (MLC) phosphorylation and shape change through targeting the RhoA-Rho kinase-MLC phosphatase signaling pathway. *Blood.* 2013;122 (20):3533-3545.
27. Coort SLM, Willems J, Coumans WA, et al. Sulfo-N-succinimidyl esters of long chain fatty acids specifically inhibit fatty acid translocase (FAT/CD36)-mediated cellular fatty acid uptake. *Mol Cell Biochem.* 2002;239(1-2):213-219.
28. Ashraf MZ, Kar NS, Chen X, et al. Specific oxidized phospholipids inhibit scavenger receptor bi-mediated selective uptake of cholesteryl esters. *J Biol Chem.* 2008;283(16):10408-10414.
29. Zimman A, Titz B, Komisopoulou E, Biswas S, Graeber TG, Podrez EA. Phosphoproteomic analysis of platelets activated by pro-thrombotic oxidized phospholipids and thrombin. *PLoS ONE.* 2014;9(1):e84488.
30. Csányi G, Cifuentes-Pagano E, Al Ghouleh I, et al. Nox2 B-loop peptide, Nox2ds, specifically inhibits the NADPH oxidase Nox2. *Free Radic Biol Med.* 2011;51(6):1116-1125.
31. Lassègue B, San Martín A, Griendling KK. Biochemistry, physiology, and pathophysiology of NADPH oxidases in the cardiovascular system. *Circ Res.* 2012;110(10):1364-1390.
32. Huang MM, Bolen JB, Barnwell JW, Shattil SJ, Brugge JS. Membrane glycoprotein IV (CD36) is physically associated with the Fyn, Lyn, and Yes protein-tyrosine kinases in human platelets. *Proc Natl Acad Sci USA.* 1991;88(17): 7844-7848.
33. Isenberg JS, Romeo MJ, Yu C, et al. Thrombospondin-1 stimulates platelet aggregation by blocking the antithrombotic activity of nitric oxide/cGMP signaling. *Blood.* 2008; 111(2):613-623.
34. Murthy KS, Zhou H, Grider JR, Makhlouf GM. Inhibition of sustained smooth muscle contraction by PKA and PKG preferentially mediated by phosphorylation of RhoA. *Am J Physiol Gastrointest Liver Physiol.* 2003;284(6): G1006-G1016.
35. Butt E, Abel K, Krieger M, et al. cAMP- and cGMP-dependent protein kinase phosphorylation sites of the focal adhesion vasodilator-stimulated phosphoprotein (VASP) in vitro and in intact human platelets. *J Biol Chem.* 1994;269(20): 14509-14517.

36. Csányi G, Gajda M, Franczyk-Zarow M, et al. Functional alterations in endothelial NO, PGI_2 and EDHF pathways in aorta in ApoE/LDLR-/- mice. *Prostaglandins Other Lipid Mediat.* 2012;98(3-4): 107-115.

37. Kuijpers MJE, de Witt S, Nergiz-Unal R, et al. Supporting roles of platelet thrombospondin-1 and CD36 in thrombus formation on collagen. *Arterioscler Thromb Vasc Biol.* 2014;34(6): 1187-1192.

38. Ghosh A, Li W, Febbraio M, et al. Platelet CD36 mediates interactions with endothelial cell–derived microparticles and contributes to thrombosis in mice. *J Clin Invest.* 2008;118(5):1934-1943.

39. Zhu W, Li W, Silverstein RL. Advanced glycation end products induce a prothrombotic phenotype in mice via interaction with platelet CD36. *Blood.* 2012;119(25):6136-6144.

40. Wang Y, Fang C, Gao H, et al. Platelet-derived S100 family member myeloid-related protein-14 regulates thrombosis. *J Clin Invest.* 2014;124(5): 2160-2171.

41. Chen K, Li W, Major J, Rahaman SO, Febbraio M, Silverstein RL. Vav guanine nucleotide exchange factors link hyperlipidemia and a prothrombotic state. *Blood.* 2011;117(21):5744-5750.

42. Chan H-C, Ke L-Y, Chu C-S, et al. Highly electronegative LDL from patients with ST-elevation myocardial infarction triggers platelet activation and aggregation. *Blood.* 2013;122(22): 3632-3641.

43. Aviram M. Modified forms of low density lipoprotein affect platelet aggregation in vitro. *Thromb Res.* 1989;53(6):561-567.

44. Assinger A, Koller F, Schmid W, Zellner M, Koller E, Volf I. Hypochlorite-oxidized LDL induces intraplatelet ROS formation and surface exposure of CD40L—a prominent role of CD36. *Atherosclerosis.* 2010;213(1):129-134.

45. Massberg S, Sausbier M, Klatt P, et al. Increased adhesion and aggregation of platelets lacking cyclic guanosine 3′,5′-monophosphate kinase I. *J Exp Med.* 1999; 189(8):1255-1264.

46. Naseem KM. The role of nitric oxide in cardiovascular diseases. *Mol Aspects Med.* 2005;26(1-2):33-65.

47. Pignatelli P, Carnevale R, Di Santo S, et al. Inherited human gp91phox deficiency is associated with impaired isoprostane formation and platelet dysfunction. *Arterioscler Thromb Vasc Biol.* 2011;31(2):423-434.

48. Stellos K, Sauter R, Fahrleitner M, et al. Binding of oxidized low-density lipoprotein on circulating platelets is increased in patients with acute coronary syndromes and induces platelet adhesion to vascular wall in vivo—brief report. *Arterioscler Thromb Vasc Biol.* 2012;32(8): 2017-2020.